Systems & Control Transactions

Original Research Article
Peer Reviewed Conference Proceeding
ESCAPE 36 - European Symposium on Computer Aided Process Engineering
Sheffield, UK. 21-24 June 2026

PSE PRESS

Experiments & Modelling of Batch Fermentation of *Fusarium venenatum* on Glucose-Fructose Mixtures

Tom Vinestock[a], Miao Guo[a]*

[a] King's College London, Department of Engineering, London, United Kingdom
* Corresponding Author: miao.guo@kcl.ac.uk

ABSTRACT

Single-cell protein (SCP) fermentation efficiently converts carbohydrates into high-protein food products but typically relies on purified glucose. Better understanding of SCP growth on mixed sugar substrates could allow for use of lower-cost, less processed sugars and waste-derived feedstocks. Glucose–fructose mixtures are particularly relevant, as these are the main sugars in sucrose hydrolysates and are also common in many food and beverage waste streams. In this study, the growth of *Fusarium venenatum* on glucose–fructose mixtures was investigated experimentally and modelled using a lagged dual-substrate Monod framework incorporating inhibition of fructose growth by glucose. Batch fermentations were conducted at a fixed total sugar concentration (15 g/L) with four different initial substrate compositions. Model parameters were estimated using both single-experiment and multi-experiment fitting strategies using differential evolution and wild bootstrap uncertainty analysis. A shared parameter set reproduced biomass growth and substrate depletion across all conditions with only a modest increase in prediction error relative to individual fits. Bootstrap analysis revealed substantial correlation among uptake and inhibition parameters, while yield coefficients were well constrained. These results demonstrate that mixed-sugar growth of *F. venenatum* can be described using a unified kinetic model, supporting the feasibility of transitioning from glucose-only to mixed-substrate SCP fermentation.

Keywords: Batch Process, Biomass, Biosystems, Fermentation, Modelling and Simulations, Single Cell Protein, Dual Substrate Growth

BACKGROUND

Single-cell protein (SCP) fermentation provides an efficient route for converting carbohydrate into high-protein food products and has the potential to reduce land use, greenhouse gas emissions, and resource intensity relative to conventional animal-based protein production [1]. Among SCP microorganisms, filamentous fungi such as *Fusarium venenatum* are of particular industrial interest because their mycelial morphology imparts a fibrous, meat-like texture desirable in food applications [2]. Industrial SCP processes commonly rely on refined carbohydrate feedstocks, most commonly glucose [3]. However, the use of single, purified substrates increases upstream processing requirements and cost and limits the flexibility of fermentation systems to utilise heterogeneous, low-cost and waste-derived carbon sources [4].

There are many potential feedstocks that are composed of mixtures of sugars rather than a single monosaccharide. Glucose–fructose mixtures are especially relevant, because sucrose hydrolysates and many sugar-rich food and beverage waste streams, including fruit-processing and soft-drink manufacturing waste streams are rich in these monosaccharides [5]. When glucose and fructose are both present, there will be an interaction between their metabolisms. Quantifying this interaction is essential for constructing accurate growth models and therefore, for the rational design of fermentation strategies based on mixed-sugar feedstocks.

In this work, we estimate the parameters of a dual-substrate growth model describing the growth of *F. venenatum* on glucose–fructose mixtures. By explicitly characterising mixed-substrate kinetics, this study provides a basis for assessing the feasibility of transitioning from glucose-based operation to mixed-sugar fermentation and so supports the development of more flexible, sustainable and economically robust SCP production

processes. This will help to inform industrial process design and operation, helping to derisk the transition to dual substrate fermentation, from existing glucose-based processes.

METHODOLOGY

Experimental Methodology

50 ml of fermentation media, as defined in Table 2, was transferred into a 250 ml baffled flask. Total sugar concentration was fixed at 15 g/L. Four different initial substrate compositions were investigated: 15 g/L glucose, 10 g/L glucose + 5 g/L fructose, 5 g/L glucose + 10 g/L fructose, and 15 g/L fructose. This was then inoculated with *F. venenatum* A3/5 spores to give an initial spore concentration of 10, 000/ml in each flask. Spores were generated by inoculating a 30g/l glucose/low-nitrogen RHM media with a plate culture provided by Quorn Foods, incubating this broth in a shaker-incubator at 28°C for 4 days, and then straining to remove fungal filaments.

To ensure sufficient oxygen transfer to the fermentation broth, oxygen and compressed air were blended to give a headspace oxygen concentration of 200% of the oxygen concentration of air (~42% oxygen by volume). This enriched air was humidified before it entered the fermentation flask to prevent evaporation losses. The oxygen flow rate was ~0.2 LPM and the air flow rate was ~0.5 LPM, for a total flow rate of ~0.7 LPM, or ~0.2 LPM /flask. This is substantially in excess of metabolic requirements, meaning that the headspace gas composition should remain unchanged during the fermentation. The flasks were vented to maintain atmospheric pressure throughout the fermentation.

PreSens SFR vario readers (PreSens, Germany) were used to measure biomass concentration, pH, and broth dissolved oxygen concentration during the fermentation runs. The biomass concentration measure is based on the reflectance of the fermentation broth, while pH and dissolved oxygen are determined based on pre-calibrated optical sensor spots. Biomass and pH concentration were recalibrated after each experiment using the start and end points. At the endpoint, to determine the biomass concentration, the fermentation broth from each flask was vacuum filtered through a pre-dried, pre-weighed fine fibre-glass filter. It was then rinsed with deionised water and then dried to constant mass in a 65 °C oven, before the filter was reweighed using a precision balance.

Each experiment was conducted in triplicate. During each run, 300 µL samples were collected from the flasks at regular intervals, with sampling concentrated in the exponential growth phase, for substrate analysis by high-performance liquid chromatography (HPLC). The HPLC parameters are given in Table 3. Before the fermentation experiments, the linear relationship between peak area and substrate concentration was confirmed, and calibration curves for glucose and fructose were established over the full concentration ranges observed. The fermentation was allowed to continue until HPLC analysis showed the sugar substrates had been fully depleted.

Oxygen uptake rate (OUR) was calculated according to Equation 1, where kLa is the volumetric mass transfer coefficient, C_{O_2} is the measured dissolved oxygen concentration in the fermentation broth, and $C^*_{O_2}$ is the equilibrium dissolved oxygen concentration based on Henry's Law. kLa was determined using the gassing-out method, in which dissolved oxygen was first reduced to near zero by nitrogen sparging and then monitored during re-aeration using a PreSens DO sensor.

$$OUR = kLa * (C^*_{O_2} - C_{O_2}) \quad (1)$$

Biomass growth rate was estimated by applying a Savitzky–Golay differentiating filter [6] to the biomass concentration time series, in order to reduce the effect of noise in the biomass concentration measurement. The specific growth rate was estimated by linear regression of $ln(X)$ against time within a centred sliding window, where X is the biomass concentration, with the local slope taken as the instantaneous growth rate.

Table 1: Experimental Parameters

Parameter	Value
Broth Volume	50 ml
Shaker Orbit	20 mm
Shaker Rotational Speed	220 RPM
Incubation Temperature	28 °C
Headspace Oxygen Concentration	200 % air saturation
Volumetric Mass Transfer Coefficient (kLa)	96 /h

Table 2: Fermentation Media Components

Media Component	Amount per Flask (ml)
Rank Hovis McDougal Media (RHM) [7] with 30 g/l KH_2PO_4	46
Polypropylene Glycol (5% w/w) Solution	0.5
Tween-80 (1% w/w) Solution	0.5
Glucose (25% w/v)	3-x
Fructose (25% w/v)	x
$x \in \{0, 1, 2, 3\}$	

Figure 1. Photograph of experimental set-up. The blue base units are the PreSens Shake Flask Readers. The media bottles visible on the right humidify the enriched air before it enters the baffled flasks.

Table 3: HPLC Parameters

Parameter	Value
Column	Bio-Rad Aminex HPX-87H
Detector	Shimadzu RID-20A
Mobile Phase	0.001 M H_2SO_4
Run Time	35 min
Column Temperature	30°C
Flow Rate	0.4 mL/min
Injection Volume	5 mL

Computational Methodology

Biomass growth was modelled using a lagged dual-substrate Monod [8] framework, with glucose assumed to be the preferred substrate. Accordingly, the model includes inhibition of fructose utilisation by glucose, but no inhibition of glucose utilisation by fructose. During the lag phase of duration λ, biomass growth and substrate consumption were assumed to be negligible, such that $\dot{X} = \dot{S}_1 = \dot{S}_2 = 0$. After the end of the lag phase, the system dynamics are given by:

$$\dot{X} = (\mu_1 + \mu_2) X \tag{2}$$

$$\dot{S}_1 = \frac{-\mu_1}{Y_1} X \tag{3}$$

$$\dot{S}_2 = \frac{-\mu_2}{Y_2} X \tag{4}$$

with specific growth rates:

$$\mu_1 = \mu_{max,1} \frac{S_1}{S_1 + K_{S1}} \tag{5}$$

$$\mu_2 = \mu_{max,2} \frac{S_2}{S_2 + K_{S2}} \frac{1}{1 + \frac{S_1}{K_I}} \tag{6}$$

Here, X denotes biomass concentration, $S_1$and S_2 are the concentrations of glucose and fructose, respectively, $\mu_{\max,1}$ and $\mu_{\max,2}$ are the maximum specific growth rates, $K_{S1}$and $K_{S2}$are the Monod half-saturation constants, K_I is the glucose inhibition constant for fructose growth and $Y_1$and Y_2 are yield coefficients. A step-function lag phase, as described in [9], was included to account for delayed onset of growth. The $\frac{1}{1+\frac{S_1}{K_I}}$ term models catabolite repression of fructose by glucose, as in [10]. Note that K_I is the minimum glucose concentration sufficient to halve the fructose-related specific growth rate, μ_2. Therefore, smaller values of K_I indicate stronger inhibition.

Model parameters were estimated using two fitting strategies: (i) individual fits to each experiment, and (ii) a combined multi-experiment fit. In the multi-experiment fit, seven kinetic parameters ($\mu_{\max,1}, \mu_{\max,2}, K_{S1}, K_{S2}, K_I, Y_1,$ and Y_2) were constrained to be identical across all four experiments, while the lag time and initial biomass concentration were estimated separately for each experiment, giving a total of 15 fitted parameters. The values obtained from this shared-parameter fit were subsequently compared with those obtained from the single-experiment fits to assess the consistency and robustness of the kinetic estimates.

Parameter estimation was performed by minimising a weighted sum of squared errors across biomass and substrate measurements from triplicate flasks. To account for the higher sampling frequency of biomass measurements relative to substrate measurements, substrate residuals were weighted by $w_S = \frac{n_X}{n_S}$, where n_X is the number of biomass measurements and n_S is the total number of substrate measurements. This weighting equalises the aggregate contribution of the substrate data to that of the biomass data.

Equation 7 defines the single-flask error, with $i \in \{1, \dots, 4\}$ indexing the initial substrate condition, $f \in \{1, 2, 3\}$ the flask replicate, k the biomass observation time index, and j the substrate observation time index. The error for each initial substrate condition was then $E_{\mathrm{i}} = \sum_{f=1}^{3} E_i$. This is used as the objective function for the single experiment fit. For the multi-experiment fit, the objective function was $E_{\mathrm{tot}} = \sum_{i=1}^{4} E_i$.

$$E_{i,f} = \sum_{k=0}^{n_x-1} \left(X_{i,f}^{pred}[k] - X_{i,f}^{obs}[k] \right)^2 + \sum_{j=0}^{n_s-1} w_s \left(S_{i,f,1}^{pred}[j] - S_{i,f,1}^{obs}[j] \right)^2 + \sum_{j=0}^{n_s-1} \mathrm{w_s} \left(S_{i,f,2}^{pred}[j] - S_{i,f,2}^{obs}[j] \right)^2 \tag{7}$$

Table 4: Kinetic Parameter Bounds

Parameter	Lower Bound	Upper Bound	Type	Unit
$\mu_{max,1}$	0.01	0.6	Global for shared fit	/h
$\mu_{max,2}$	0.01	0.6		/h
K_{S1}	0.001	5.0		g/L
K_{S2}	0.001	5.0		g/L
K_I	0.001	5.0		g/L
Y_1	0.01	1.0		g/g
Y_2	0.01	1.0		g/g
λ	0	60.0	Experiment specific	h
X_0	0	0.5		g/L

Optimisation was performed using differential evolution as implemented in SciPy [11], using the best1bin strategy, a population size of 50, mutation dithering over [0.5, 1.0], and a crossover probability of 0.7, followed by local polishing with L-BFGS-B. The bounds used for each parameter are set out in Table 4.

Confidence intervals for the parameter estimates were constructed using the wild bootstrap method [12], which does not require the assumption of homoscedastic residuals. Per-observation residuals were first computed from the fitted model on the original data. For each of 50 bootstrap replicates, a synthetic response dataset $y_n^*$was generated by adding randomly signed residuals to the model fitted values. Specifically, if $\hat{y}_n$ denotes the predicted value at observation n and $\hat{e}_n = y_n - \hat{y}_n$the corresponding residual, then the bootstrap data were constructed as $y_n^* = \hat{y}_n + w_n\hat{e}_n$, where $w_n \in \{-1, +1\}$ is a Rademacher random variable taking each value with equal probability. This procedure preserves the magnitude and structure of the original residuals while randomly reversing their sign, thereby maintaining the mean trend and accommodating heteroscedastic error behaviour. Each synthetic dataset was then re-fitted using the same differential evolution procedure, and the distribution of the resulting parameter estimates across all replicates was used to construct 95% bootstrap confidence intervals.

RESULTS & DISCUSSION

Experimental Results & Discussion

The experimental results in Figure 2 show good repeatability within an experiment, particularly for the substrate and biomass concentrations, as well as pH. There are greater differences between replicates for oxygen concentration, oxygen uptake rate (OUR), biomass growth rate and specific growth rate. With respect to biomass growth rate and specific growth rate (SGR), part of this is probably due to noise in the biomass concentration readings. However, despite this, many of the results are as would be expected: the peak OUR and SGR are highest for the pure glucose substrate, and monotonically reduce as the initial glucose concentration is reduced in favour of fructose. The SGR results suggest, in contrast to the lag model, which assumes that SGR is maximum at the very start of the exponential growth phase, that there is a gradual ramp up in SGR, until the falling substrate concentrations begin to reduce SGR again.

The length of the lag phase doesn't follow the expected pattern, with a shorter lag phase for the fructose-glucose mixture than for the pure glucose. This is believed to be driven by differences in the age and viability of the inoculation conidia.

The HPLC results show some anomalies, with the substrate concentrations not always monotonically decreasing with time. This could be due to heterogeneity in the fermentation broth, or HPLC-related factors such as peak overlap with other broth components, baseline drift, or small variations in sample preparation and integration that introduce apparent fluctuations in the measured concentrations.

Computational Results & Discussion

The MAE for the multi-experiment fit was larger than that of the single-experiment fits, as expected due to the reduced number of free parameters. However, despite the single-experiments fit providing many more degrees of freedom, since the single-experiment fits allow independent estimation of kinetic parameters for each dataset, whereas the multi-experiment fit enforces a shared parameter set, the difference in the magnitude of the MAE between the two is slight, at c. 30% higher total MAE for the multi-experiment fit compared to the single experiment fit. MAE for the multi-experiment is still below 0.5 g/l.This suggests that the model is flexible enough to describe growth rates with various initial glucose and fructose concentration, without requiring re-estimation of kinetic parameters for each initial condition. From a process modelling perspective, this supports the use of a globally parameterised model for predictive simulations and control design.

Figure 4 shows that there is considerable variation in the single experiment parameter estimates, suggesting weak identifiability from individual datasets, particularly as some of the parameters estimated based on single experiments seem to be outside the plausible range. For example, the Y_2 estimate from the Glu 10 g/l + Fru 5 g/l is nearly 1. The parameters estimated on data from all four experiments are more reliable. However, the $K_{S,1}$estimate would be expected to be smaller than the $K_{S,2}$estimate, as glucose is the favoured substrate.

Comparison of the median $\mu_{\max,1}$and $\mu_{\max,2}$ estimates (Figures 4 and 6) with the observed specific growth rates under pure glucose and pure fructose

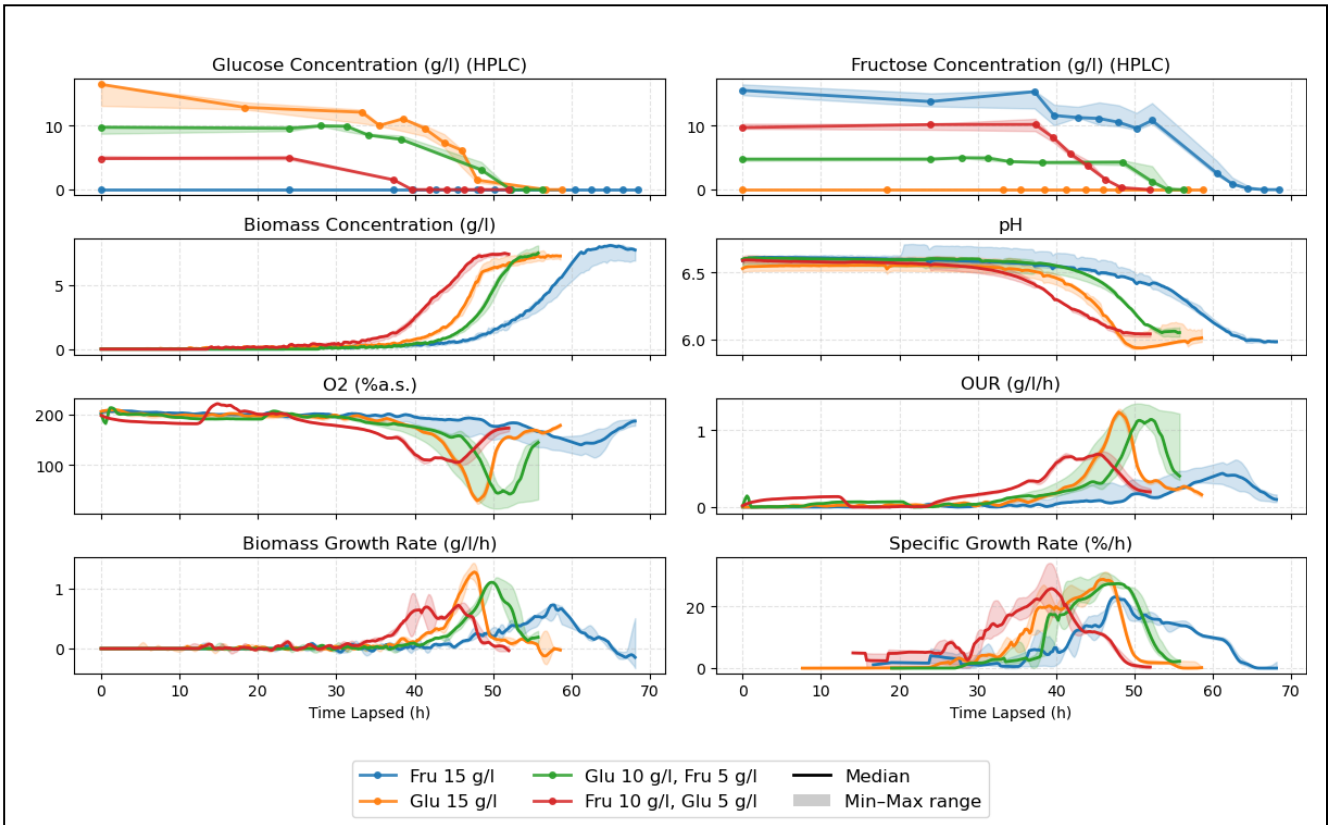

Figure 2. Experimental results for glucose-fructose mixed-substrate batch fermentations. Substrate and biomass concentrations, as well as pH and O_2, were directly measured. OUR, biomass growth rate and specific growth rate were calculated based on the measurements as explained in the Methodology.

conditions (Figure 2) shows that the peak specific growth rates exceed the corresponding estimates. This reflects the modelling assumption of a step change in growth rate at the end of the lag phase, which is not supported by the data. Instead, the specific growth rate increases gradually to a maximum, leading to underestimation of the true peak growth rate by $\mu_{\max,1}$and $\mu_{\max,2}$.

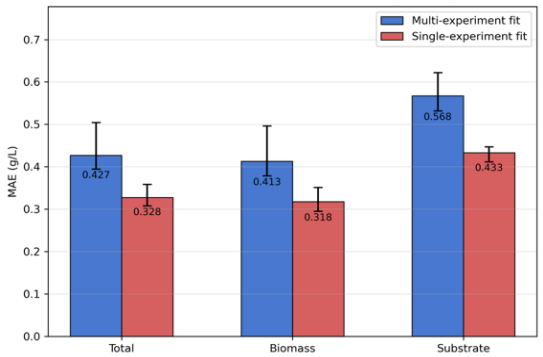

Figure 3. Mean absolute error (MAE) of multi-experiment and single-experiment model fits evaluated against observed biomass and substrate concentrations. Bar heights represent the median MAE across 20 wild bootstrap replicates and error bars denote the 95% confidence interval.

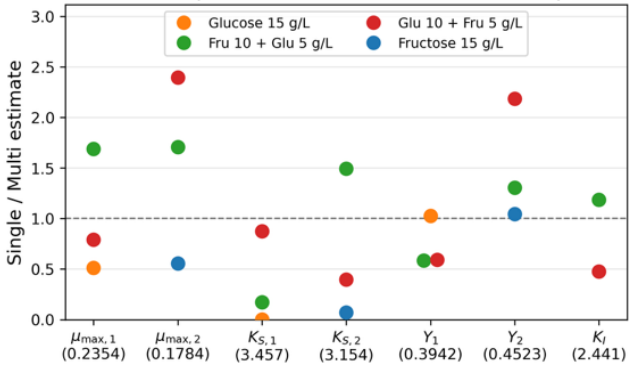

Figure 4. Single-experiment parameter estimates (median of 20 bootstrap replicates) for each experimental condition, normalised by the corresponding multi-experiment estimate (median of bootstrap replicates). A value of unity indicates agreement between the two fitting approaches.

Importantly, the multi-experiment model reproduces the qualitative and quantitative features of the growth and substrate depletion dynamics across all 4 experiments (Figure 5), capturing the timing and shape of the exponential growth phase and the coupled consumption of glucose and fructose. Deviations between the

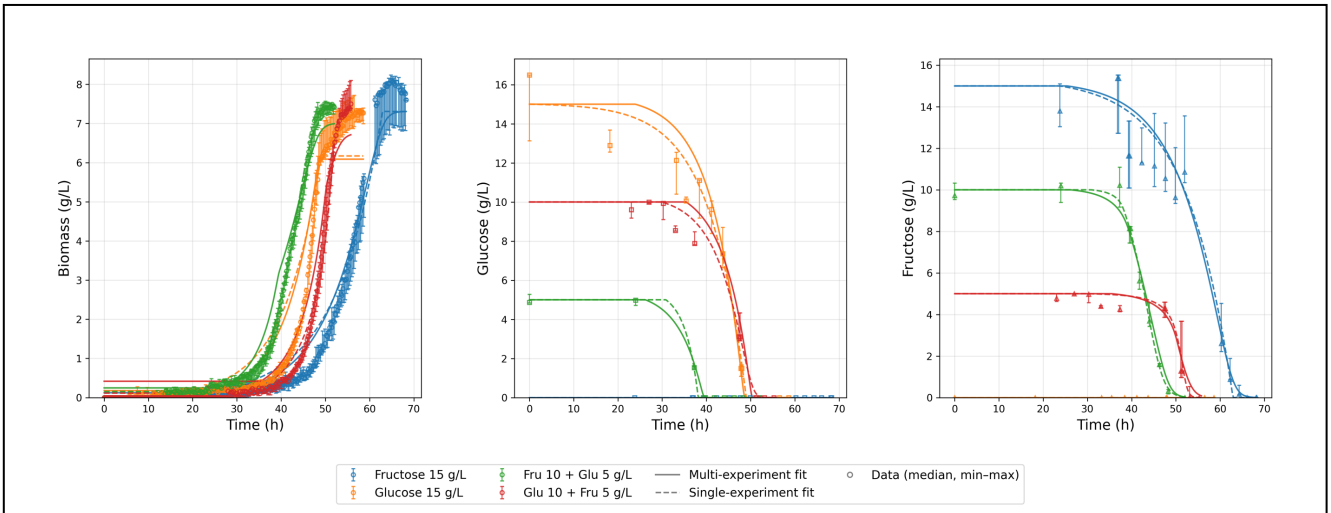

Figure 5. Comparison of single-experiment and multi-experiment model fits against original experimental data for a lagged dual-substrate Monod kinetic model, for batch fermentation across 4 different initial substrate conditions.

model predictions from the shared parameters and the experiment-specific parameters are generally small.

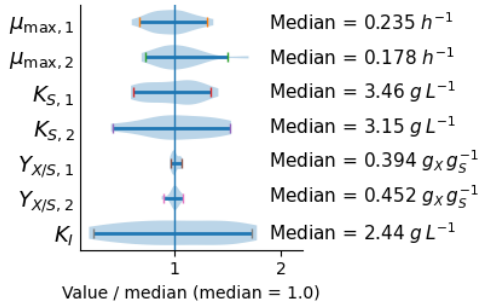

Figure 6. Median value and 95% confidence intervals for glucose-fructose dual substrate growth parameters based on wild bootstap method with 20 replicates.

The bootstrap results show considerable residual uncertainty in many of the parameter estimates. With the exception of the two yield coefficients, the redundancy in the model and the limited amount of substrate concentration data make it difficult to disentangle the effects of $\mu_{\max,1}$ and $K_{S,1}$ in the case of glucose growth, and $\mu_{\max,2}$, $K_{S,2}$ and K_I in the case of fructose growth. This can be seen in the Spearman Correlation Heatmap, which shows strong positive correlation between $\mu_{\max,1}$ and $K_{S,1}$, as well as $\mu_{\max,2}$ and $K_{S,2}$, and strong negative correlation between K_I and both $\mu_{\max,2}$ and $K_{S,2}$. As a result, the observed fructose uptake can be equivalently explained by a reduced $\mu_{\max,2}$, a high effective $K_{S,2}$, or strong glucose inhibition (low K_I), limiting mechanistic interpretability of the fitted parameters.

CONCLUSION

This study investigated the growth of *F. venenatum* on glucose–fructose mixtures and quantified the associated kinetics using a lagged dual-substrate Monod model with glucose inhibition of fructose utilisation. Although noise in derived rates and minor non-monotonicity in HPLC measurements introduced uncertainty, the overall trends were reproducible across replicates and aligned with expected physiological behaviour. Notably, the specific growth rate exhibited a gradual increase during early exponential growth rather than an instantaneous maximum, indicating that a strict step-change assumption at the end of the lag phase may be an oversimplification of the underlying dynamics.

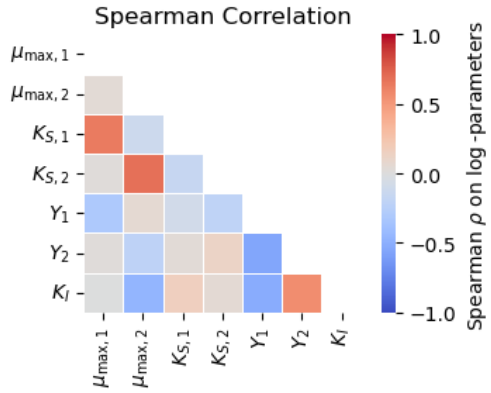

Figure 7. Heatmap of pairwise Spearman rank correlation coefficients between kinetic parameter estimates across wild bootstrap replicates, indicating the degree of parameter interdependence in the fitted model.

Parameter estimation using both single-experiment and multi-experiment fitting demonstrated that a common set of kinetic parameters can describe growth across a range of initial substrate compositions with only a modest loss of accuracy relative to individually fitted models. This supports the suitability of a unified dual-

substrate framework for representing mixed-sugar growth in *F. venenatum*. Wild bootstrap analysis revealed substantial uncertainty and correlation among several kinetic parameters, particularly those governing fructose uptake and inhibition, reflecting structural redundancy in the model and limited resolution in the available substrate data. By contrast, yield coefficients were comparatively well identified, suggesting that overall carbon conversion efficiency is more robustly constrained than individual uptake kinetics.

Together, these results provide quantitative evidence that glucose–fructose mixtures can be modelled within a mechanistic kinetic framework and that mixed-substrate operation can be described without re-parameterising the model for each feed composition.

This contributes to the development of predictive tools for SCP fermentations using heterogeneous sugar streams and supports the feasibility of transitioning from glucose-only processes to mixed-sugar feedstocks.

FUTURE WORK

Future work will investigate the applicability of this model to continuous fermentation of *F. venenatum* on glucose-fructose mixtures. This is a more industrially relevant mode of operation, and will help to address the key question of whether significant simultaneous co-utilisation of glucose and fructose can be realised in industrially relevant conditions.

ACKNOWLEDGEMENTS

The authors gratefully acknowledge funding from Quorn and the BBSRC, under project reference 2725958. Additionally, the authors would like to thank Mark Taylor (Quorn Foods) for technical advice, and material support, such as access to the *F. venenatum* A3/5 strain.

AUTHOR IDENTIFIERS

Author ORCIDs:
Vinestock T: 0009-0002-7689-2837
Guo M: 0000-0001-7733-5077

REFERENCES

1. Good Food Institute, Fermentation: State of the industry report. (2024)
2. Finnigan TJA, Theobald HE, Bajka B. Mycoprotein: a healthy and sustainable source of alternative protein-based foods. Annual Review of Food Science and Technology 16:105-125 (2025). https://doi.org/10.1146/annurev-food-111523-121802
3. Yang Z, Li L, Chen Y, Zhu L, Zhu Z, Jiang L. Trends in customizable single-cell protein production enabled by synthetic biology: carbon-negative biomanufacturing and engineered functionalities. J. Agric. Food Chem. 73:32957-32969 (2025). https://doi.org/10.1021/acs.jafc.5c08537
4. Vlaeminck E, Uitterhaegen E, Quataert K, Delmulle T, De Winter K, Soetaert WK. Industrial side streams as sustainable substrates for microbial production of poly(3-hydroxybutyrate) (PHB). World J Microbiol Biotechnol 38: (2022). https://doi.org/10.1007/s11274-022-03416-z
5. Thiviya P, Gamage A, Kapilan R, Merah O, Madhujith T. Single cell protein production using different fruit waste: a review. Separations 9:178 (2022). https://doi.org/10.3390/separations9070178
6. Savitzky A, Golay MJE. Smoothing and differentiation of data by simplified least squares procedures.. Anal. Chem. 36:1627-1639 (2002). https://doi.org/10.1021/ac60214a047
7. Whittaker JA. Sugar, soil and sequencing: Studies in *Fusarium venenatum*. PhD Thesis, Univ Nottingham (2022) https://repository.nottingham.ac.uk/handle/123456789/59078
8. Monod J. The growth of bacterial cultures. Annu Rev Microbiol 3:371-394 (1949). https://doi.org/10.1146/annurev.mi.03.100149.002103
9. Buchanan RL, Whiting RC, Damert WC. A comparison of the Gompertz, Baranyi, and three-phase linear models for fitting bacterial growth curves. Int J Food Microbiol 36(2–3):151–159 (1997) https://doi.org/10.1016/S0168-1605(97)01286-6
10. Schmitt E, Bura R, Gustafson R, Ehsanipour M. Kinetic modeling of moorella thermoacetica growth on single and dual-substrate systems. Bioprocess Biosyst Eng 39:1567-1575 (2016). https://doi.org/10.1007/s00449-016-1631-8
11. Virtanen P, et al. SciPy 1.0: fundamental algorithms for scientific computing in Python. Nat Methods 17:261–272 (2020) https://doi.org/10.1038/s41592-019-0686-2
12. Wu CFJ. Jackknife, bootstrap and other resampling methods in regression analysis. Ann Stat 14(4):1261–1295 (1986) http://www.jstor.org/stable/2241454.